C. R. Mecanique 344 (2016) 582–595

Contents lists available at ScienceDirect

Comptes Rendus Mecanique

www.sciencedirect.com

Equivalent Liénard-type models for a fluid transmission line

Modèles équivalents de type Liénard pour une ligne de transmission de fluides

Lizeth Torres [a,b,*], Jorge Alejandro Delgado Aguiñaga [c], Gildas Besançon [d,e], Cristina Verde [a], Ofelia Begovich [c]

[a] *Instituto de Ingeniería, Universidad Nacional Autónoma de México, 04510, Coyoacán, Mexico City, Mexico*
[b] *Cátedras CONACYT, Mexico*
[c] *Centro de Investigación y de Estudios Avanzados CINVESTAV Unidad Guadalajara, 45019 Zapopan, Jalisco, Mexico*
[d] *Université Grenoble Alpes, GIPSA-Lab, 38000 Grenoble, France*
[e] *CNRS, GIPSA-Lab, 38000 Grenoble, France*

ARTICLE INFO

Article history:
Received 2 March 2016
Accepted 13 April 2016
Available online 17 May 2016

Keywords:
Pipelines
Fluid dynamics
Liénard equation
State observers
Parameter identification

Mots-clés :
Canalisations
Dynamique des fluides
Équation de Liénard
Observateurs d'états
Identification de paramètres

ABSTRACT

The main contribution of this paper is the derivation of spatiotemporal Liénard-type models for expressing the dynamical behavior of a fluid transmission line. The derivation is carried out from a quasilinear hyperbolic system made of a momentum equation and a continuity one. An advantage of these types of models is that they are suitable for formulating estimation algorithms. This claim is confirmed in the present paper for the case of fluid dynamics, since the article presents the conception and evaluation of a Liénard model-based observer that estimates the parameters of a pipeline such as the friction factor, the equivalent length and the wave speed. To show the potentiality of the approach, results based on some simulation and experimental tests are presented.

RÉSUMÉ

Cet article envisage principalement la dérivation de modèles de type Liénard pour exprimer le comportement dynamique d'une ligne de transmission de fluides. Le calcul est effectué à partir d'un système hyperbolique quasi linéaire constitué d'une équation de quantité de mouvement et d'une équation de continuité. Dans des études précédentes, il a été montré que transformer les systèmes régis par une équation différentielle de type $\ddot{x}(t) + F_0(x(t))\dot{x}(t) + G_0(x(t)) = 0$ dans la forme de Liénard peut s'avérer utile à la conception d'algorithmes d'estimation. Cette affirmation est confirmée dans cet article pour le cas des fluides, car la conception et l'évaluation d'un observateur basé sur un modèle de

* Corresponding author.
E-mail addresses: ftorreso@iingen.unam.mx (L. Torres), adelgado@gdl.cinvestav.mx (J.A.D. Aguiñaga), Gildas.Besancon@grenoble-inp.fr (G. Besançon), verde@unam.mx (C. Verde), obegovi@gdl.cinvestav.mx (O. Begovich).

http://dx.doi.org/10.1016/j.crme.2016.04.004
1631-0721/

type Liénard, estimant les paramètres d'une canalisation, y sont présentées. L'approche est illustrée par des résultats de tests en simulation et expérimentaux.

1. Introduction

The so-called *Liénard equation* is a second-order differential equation proposed by physicist Alfred-Marie Liénard to study sustained oscillations and widely used to model biological and physical systems. Some examples of studies using the Liénard equation are listed in Table 1.

In the present paper, the topic of interest is the *dynamical modeling of fluid transmission lines*. This comes in continuation of a preliminary study of [1], where a Liénard-type model was introduced in terms of the flow rate in the line, and some so-called *state observer* was proposed based on it. The motivation for such a work was to obtain a suitable model for the design of parameter-identification algorithms for pipelines, which are themselves important for monitoring purposes, since actual parameters usually differ from the design values because of manufacturing, installation, operation, and ageing of each single pipe. Therefore, in order to design algorithms based on the pipeline dynamics, such as diagnosis, control, or prognosis systems, it is necessary to develop methodologies to continuously update the pipeline parameters (as in [2–4] for instance).

The present article can thus be considered as an extension of [1], with the following novelties: (1) an extension of flow-based Liénard-type modeling to some pressure-based case (hybrid model); (2) an emphasis on a unified linearized model either in terms of the flow rate or in terms of the pressure head; (3) an example of an application to estimation via the construction of an exponential boundary observer based on the flow rate model to simultaneously estimate the friction and the equivalent length of a pipeline; (4) an exponential observer based on the unified linearized model to simultaneously estimate the friction and the wave speed.

The paper is thus organized as follows: Section 2 first recalls the Liénard equation with the related Liénard transform. Section 3 recalls the basic hydraulic equations for fluid dynamics in a pipeline and then shows how to turn those hydraulic equations into some Liénard-type models, either in terms of flow rate or in terms of pressure head. Section 4 subsequently presents the proposed Liénard-based observer approach for parameter estimation in a pipeline, as well as related illustrative simulation and experimental results. Section 6 finally ends the paper with some conclusions and perspectives.

Table 1
Application of Liénard equation.

Biological modeling
Biochemical reactions [5]. Heart dynamics [6]. Diseases [7]. Neuron dynamics [8–10]. Fermentation [11].
Mathematics
Bifurcation theory [12]. Fixed point theory [13]. Existence and uniqueness of limit cycles [14]. Hilbert's 16th problem [15].
Vibration and electronic theory
Voltage-controlled oscillators [16].
Signal processing
Periodic signal modeling [17].

2. Recalls on Liénard's equation

A generalization of differential equations that govern the behavior of second-order mechanical systems is the so-called Liénard system [18], which corresponds to the following equation:

$$\ddot{x}(t) + F_0(x(t))\dot{x}(t) + G_0(x(t)) = 0, \qquad \text{where} \qquad \dot{x}(t) = \frac{\mathrm{d}x(t)}{\mathrm{d}t},\ \ddot{x}(t) = \frac{\mathrm{d}^2x(t)}{\mathrm{d}t^2} \tag{1}$$

for given functions F_0, G_0, and position $x(t)$.

A particular case of Eq. (1) is the equation of damped oscillations: $\ddot{x}(t)+\gamma\dot{x}(t)+\omega^2x(t)=0$, where $\ddot{x}(t)$ is the acceleration, $\dot{x}(t)$ is the velocity, and γ, ω are constant parameters. For $\gamma = 0$, the equation of the linear harmonic oscillator is obtained, which represents one of the fundamental equations of both classical and quantum physics.

The Liénard-type equation can be rewritten in a state space representation by considering $x(t), \dot{x}(t)$ as state variables $x_1(t), x_2(t) \in X$, leading to

$$\begin{aligned} \dot{x}_1(t) &= x_2(t) \\ \dot{x}_2(t) &= -F_0(x_1(t))x_2(t) - G_0(x_1(t)) \end{aligned} \tag{2}$$

If model (2) is going to be used for state and parameter estimation purposes, it is necessary to define the measured output for the design of an estimation algorithm. Hereafter, it is then considered that $y(t) = x_1(t)$, i.e., only the first state is available.

Notice that nonlinear function $F_0(x_1(t))$ is *affine* to $x_2(t)$ (an unmeasured state), which complicates the design of a possible estimator and demands a transformation to set system (2) into a more appropriate representation. An option already studied in [19] is the application of the following change of variables:

$$\begin{pmatrix} \zeta_1(t) \\ \zeta_2(t) \end{pmatrix} = \Phi \begin{pmatrix} x_1(t) \\ x_2(t) \end{pmatrix}$$

defined as

$$\Phi : \begin{pmatrix} x_1(t) \\ x_2(t) \end{pmatrix} \to \begin{pmatrix} x_1(t) \\ \dot{x}_2(t) + F(x_1(t)) \end{pmatrix} \tag{3}$$

where $F(x(t)) = \int_0^x F_0(\sigma)\,\mathrm{d}\sigma$, which transforms system (2) into

$$\begin{aligned} \dot{\zeta}_1(t) &= \zeta_2(t) - F(\zeta_1(t)) \\ \dot{\zeta}_2(t) &= -G_0(\zeta_1(t)) \\ y(t) &= \zeta_1(t) \end{aligned} \tag{4}$$

Notice that representation (4) of Eq. (1) involves now only nonlinear functions decoupled of the unmeasurable state facilitating its estimation. Furthermore, if $F(\zeta_1(t))$ and $G_0(\zeta_1(t))$ are the results of linear combinations of nonlinear function vectors $(\tilde{F}^{\mathrm{T}}(\zeta_1(t)), \tilde{G}_0{}^{\mathrm{T}}(\zeta_1(t))$ respectively) with parameter vectors θ_1 and θ_2

$$F(\zeta_1(t)) = \tilde{F}^{\mathrm{T}}(\zeta_1(t))\theta_1,\ F(\zeta_1(t)) = \tilde{G}_0^{\mathrm{T}}(\zeta_1(t))\theta_2$$

system (4) turns into

$$\begin{aligned} \dot{\zeta}_1(t) &= \zeta_2(t) - \tilde{F}^{\mathrm{T}}(\zeta_1(t))\theta_1 \\ \dot{\zeta}_2(t) &= -\tilde{G}_0^{\mathrm{T}}(\zeta_1(t))\theta_2 \\ y(t) &= \zeta_1(t) \end{aligned} \tag{5}$$

or in a more general form (assuming a possible known driving input $u(t)$) into

$$\begin{aligned} \dot{\zeta}(t) &= A_o\zeta(t) + \Phi(y(t))\theta + \varphi(u(t), y(t)) \\ y(t) &= C_o\zeta(t) \end{aligned} \tag{6}$$

with

$$A_o = \begin{pmatrix} 0 & 1 \\ 0 & 0 \end{pmatrix},\ C_0 = \begin{pmatrix} 1 & 0 \end{pmatrix}, \Phi(y(t)) = \begin{pmatrix} \tilde{F}^{\mathrm{T}}(y(t)) \\ \tilde{G}_0^{\mathrm{T}}(y(t)) \end{pmatrix}, \theta = \begin{pmatrix} \theta_1 & \theta_2 \end{pmatrix}$$

and a non-parameterized vector function $\varphi(u(t), y(t))$.

Notice that system (1) with the structure (6) now involves a linear part coupled with a regressor, which is suitable for the design of joint state and parameter estimation algorithms [20]. To show this, a particular state observer design is proposed in Section 4 to address the estimation of fluid variables in pipelines.

It is worth pointing out that the Liénard transformation (3) can be also applied to non-scalar systems or systems that depend on both space and time such as the following:

$$\ddot{x}(z,t) + F_0(x(z,t))\dot{x}(z,t) + G_0(x(z,t)) = 0 \tag{7}$$

which after the transformation turns into

$$\begin{aligned} \dot{\zeta}_1(z,t) &= \zeta_2(z,t) - F(\zeta_1(z,t)) \\ \dot{\zeta}_2(z,t) &= -G_0(\zeta_1(z,t)) \\ y(z,t) &= \zeta_1(z,t) \end{aligned} \tag{8}$$

3. Liénard-type models for fluid dynamics in pipelines

By assuming that convective changes in velocity are negligible and that both the liquid density and the cross-sectional area are constant, the momentum and continuity equations governing the dynamics of the fluid in a horizontal pipeline can be expressed as [21]:

$$\frac{\partial Q(z,t)}{\partial t} + gA_r\frac{\partial H(z,t)}{\partial z} + \frac{f}{2\phi A_r}Q(z,t)|Q(z,t)| = 0 \tag{9}$$

$$\frac{\partial H(z,t)}{\partial t} + \frac{b^2}{gA_r}\frac{\partial Q(z,t)}{\partial z} = 0 \tag{10}$$

where $(z,t) \in (0,L) \times (0,\infty)$ gathers the space [s] and time [m] coordinates respectively, L is the length of the pipe, $H(z,t)$ is the pressure head [m], $Q(z,t)$ is the flow rate [m^3/s], b is the wave speed in the fluid [m/s], g is the gravitational acceleration [m/s^2], A_r is the cross-sectional area of the pipe [m^2], ϕ is the inside diameter of the pipe [m], and f is the Darcy–Weisbach friction factor.

In this work, the initial conditions expressing the spatial profiles of $Q(z,t)$ and $H(z,t)$ at time $t=0$ are denoted by $H(z,0) = H^0(z)$, $Q(z,0) = Q^0(z)$, and two Dirichlet conditions are considered at the boundaries of the pipeline, among: (i) upstream pressure head; $H(0,t) = H_{\text{in}}(t)$; (ii) downstream pressure head, $H(L,t) = H_{\text{out}}(t)$; (iii) upstream flow rate, $Q(0,t) = Q_{\text{in}}(t)$; and (iv) downstream flow rate, $Q(L,t) = Q_{\text{out}}(t)$.

The main point of the next subsections is then to show how model (9)–(10) can be rewritten into a Liénard-like form (4).

3.1. Flow rate model

As this can be done with the telegrapher's equations, which can be arranged in terms of voltage or of current, let us here show how a representation only in terms of the flow rate can be obtained from Eqs. (9) and (10).

First, from Eq. (10), one gets

$$\frac{\partial H(z,t)}{\partial t} = -\frac{b^2}{gA_r}\frac{\partial Q(z,t)}{\partial z} \tag{11}$$

which, differentiated with respect to space, takes the following form:

$$\frac{\partial^2 H(z,t)}{\partial z\,\partial t} = -\frac{b^2}{gA_r}\frac{\partial^2 Q(z,t)}{\partial z^2} \tag{12}$$

On the other hand, by differentiating Eq. (9) with respect to time, one obtains

$$\frac{\partial^2 Q(z,t)}{\partial t^2} + gA_r\frac{\partial^2 H(z,t)}{\partial t\partial z} + \frac{f}{\phi A_r}|Q(z,t)|\frac{\partial Q(z,t)}{\partial t} = 0 \tag{13}$$

By combining the last two equations, one finally obtains:

$$\frac{\partial^2 Q(z,t)}{\partial t^2} + \frac{f}{\phi A_r}|Q(z,t)|\frac{\partial Q(z,t)}{\partial t} - b^2\frac{\partial^2 Q(z,t)}{\partial z^2} = 0 \tag{14}$$

Notice that for this equation, boundary Dirichlet conditions on $H(z,t)$ for (9)–(10) turn into Neumann conditions on $Q(z,t)$ (from Eq. (11)), and that initial conditions on $H(z,t)$, $Q(z,t)$ turn into initial conditions on $Q(z,t)$, $\partial Q(z,t)/\partial t$ (from Eq. (9)).

A classical state space realization of equation (14) is given by

$$\begin{aligned}\frac{\partial Q^a(z,t)}{\partial t} &= Q^b(z,t)\\ \frac{\partial Q^b(z,t)}{\partial t} &= -\frac{f}{\phi A_r}|Q^a(z,t)|Q^b(z,t) + b^2\frac{\partial^2 Q^a(z,t)}{\partial z^2}\end{aligned} \tag{15}$$

where $Q^a(z,t)$ and $Q^b(z,t)$ correspond to $Q(z,t)$, $\partial Q(z,t)/\partial t$, respectively. Since $Q^a(z,t)$ is the flow rate defined by $Q^a(z,t) = v(z,t)A_r$, where $v(z,t)$ is the fluid velocity and A_r the cross-sectional area of the pipeline, $Q^b(z,t)$ is directly proportional to the fluid's acceleration.

Now noting that (15) is of a form similar to (2), a transformation such as (3) can be used, which converts model (14) in a Liénard form as follows:

$$\begin{aligned}\frac{\partial Q_l^a(z,t)}{\partial t} &= Q_l^b(z,t) - \frac{f}{\phi A_r}\int^{Q_l^a}|\sigma|\,\mathrm{d}\sigma\\ \frac{\partial Q_l^b(z,t)}{\partial t} &= b^2\frac{\partial^2 Q_l^a(z,t)}{\partial z^2}\end{aligned} \tag{16}$$

which, by computing the involved integral, becomes

$$\begin{aligned}\frac{\partial Q_l^a(z,t)}{\partial t} &= Q_l^b(z,t) - \frac{f}{2\phi A_r}Q_l^a(z,t)|Q_l^a(z,t)|\\ \frac{\partial Q_l^b(z,t)}{\partial t} &= b^2\frac{\partial^2 Q_l^a(z,t)}{\partial z^2}\end{aligned} \tag{17}$$

This corresponds to the flow-based Liénard form of the pipeline dynamics.

3.2. Hybrid model (pressure head and flow rate)

The objective of this section is to discuss how a Liénard model can also be derived in terms of *pressure head*. In particular, in this case, the flow rate still remains in the dissipative term, as it will be seen.

First, by differentiating Eq. (9) with respect to space and Eq. (10) with respect to time, one has

$$\frac{\partial Q(z,t)}{\partial t \partial z} = -gA_r \frac{\partial^2 H(z,t)}{\partial z^2} - \frac{f}{2\phi A_r} \frac{\partial |Q(z,t)| Q(z,t)}{\partial z} \tag{18}$$

$$\frac{\partial^2 H(z,t)}{\partial t^2} + \frac{b^2}{gA_r} \frac{\partial Q(z,t)}{\partial t \partial z} = 0 \tag{19}$$

By substituting Eq. (18) into Eq. (19), the following second-order equation is obtained:

$$\frac{\partial^2 H(z,t)}{\partial t^2} - b^2 \frac{\partial^2 H(z,t)}{\partial z^2} - \frac{b^2 f}{g\phi A_r^2} |Q(z,t)| \frac{\partial Q(z,t)}{\partial z} = 0 \tag{20}$$

The state space representation of Eq. (20) then is

$$\begin{aligned} \frac{\partial H^a(z,t)}{\partial t} &= H^b(z,t) \\ \frac{\partial H^b(z,t)}{\partial t} &= b^2 \frac{\partial^2 H^a(z,t)}{\partial z^2} + \frac{b^2 f}{g\phi A_r^2} |Q(z,t)| \frac{\partial Q(z,t)}{\partial z} \end{aligned} \tag{21}$$

Now notice that from the continuity equation (10), one has

$$\frac{\partial Q(z,t)}{\partial z} = -\frac{gA_r}{b^2} \frac{\partial H(z,t)}{\partial t} \tag{22}$$

Hence, by substituting Eq. (22) into the second equation of system (21), one gets:

$$\begin{aligned} \frac{\partial H^a(z,t)}{\partial t} &= H^b(z,t) \\ \frac{\partial H^b(z,t)}{\partial t} &= -\frac{f}{\phi A_r} |Q(z,t)| H^b(z,t) + b^2 \frac{\partial^2 H^a(z,t)}{\partial z^2} \end{aligned}$$

similarly to (15).

At this point, the standard Liénard transformation does not apply, but one can consider the following one:

$$\begin{aligned} H_l^a(z,t) &= H^a(z,t) \\ H_l^b(z,t) &= H^b(z,t) - \int^t \frac{b^2 f}{g\phi A_r^2} |Q(z,\tau)| \frac{\partial Q(z,\tau)}{\partial z} \mathrm{d}\tau \end{aligned}$$

to get (by using again equation (22))

$$\dot{H}_l^a(z,t) = H_l^b(z,t) + \int^t \frac{b^2 f}{g\phi A_r^2} |Q(z,\tau)| \frac{\partial Q(z,\tau)}{\partial z} \mathrm{d}\tau \tag{23}$$

$$\dot{H}_l^b(z,t) = b^2 \frac{\partial^2 H_l^a(z,t)}{\partial z^2} \tag{24}$$

Here a Liénard-like model is obtained in terms of the pressure head, but still depends on the flow rate. It can yet be noticed that this form becomes similar to (17) in the case of *linearized model*, as shown below.

3.3. Linearized Liénard-type modeling

The linear versions of second-order equations (14) and (20) are

$$\frac{\partial^2 q(z,t)}{\partial z^2} = \frac{1}{b^2} \frac{\partial^2 q(z,t)}{\partial t^2} + \frac{f|Q_0|}{A_r \phi b^2} \frac{\partial q(z,t)}{\partial t} \tag{25}$$

$$\frac{\partial^2 h(z,t)}{\partial z^2} = \frac{1}{b^2} \frac{\partial^2 h(z,t)}{\partial t^2} + \frac{f|Q_0|}{A_r \phi b^2} \frac{\partial h(z,t)}{\partial t} \tag{26}$$

where q, h respectively stand for flow and pressure variations with respect to some steady state behavior defined by $H_0(z)$ and Q_0 (necessarily constant in z). With an electrical analogy, those equations can also be rewritten as

$$\frac{\partial^2 q(z,t)}{\partial z^2} = \mathcal{LC}\frac{\partial^2 q(z,t)}{\partial t^2} + \mathcal{RC}\frac{\partial q(z,t)}{\partial t} \tag{27}$$

$$\frac{\partial^2 h(z,t)}{\partial z^2} = \mathcal{LC}\frac{\partial^2 h(z,t)}{\partial t^2} + \mathcal{RC}\frac{\partial h(z,t)}{\partial t} \tag{28}$$

with $\mathcal{R} = \dfrac{f|Q_0|}{gA_r^2\phi}$, $\mathcal{L} = \dfrac{1}{gA_r}$, $\mathcal{C} = \dfrac{gA_r}{b^2}$.

Hence q and h satisfy the same equation, which means that a Liénard model can be obtained either in flow rate or in pressure head (depending on the preferred point of view), by considering the following transformations:

$$\Phi : \begin{pmatrix} q(z,t) \\ \dfrac{\partial q}{\partial t}(z,t) \end{pmatrix} \to \begin{pmatrix} \zeta_1(z,t) \\ \zeta_2(z,t) \end{pmatrix} := \begin{pmatrix} q(z,t) \\ \dfrac{\partial q}{\partial t} + \dfrac{\mathcal{R}}{\mathcal{L}} q(z,t) \end{pmatrix} \tag{29}$$

or

$$\Phi : \begin{pmatrix} h(z,t) \\ \dfrac{\partial h}{\partial t}(z,t) \end{pmatrix} \to \begin{pmatrix} \zeta_1(z,t) \\ \zeta_2(z,t) \end{pmatrix} := \begin{pmatrix} h(z,t) \\ \dfrac{\partial h}{\partial t} + \dfrac{\mathcal{R}}{\mathcal{L}} h(z,t) \end{pmatrix} \tag{30}$$

With any of those choices, Eq. (27) (or Eq. (28)) becomes

$$\frac{\partial \zeta_1(z,t)}{\partial t} = \zeta_2(z,t) - \left(\frac{\mathcal{R}}{\mathcal{L}}\right)\zeta_1(z,t) \tag{31}$$

$$\frac{\partial \zeta_2(z,t)}{\partial t} = \left(\frac{1}{\mathcal{LC}}\right)\frac{\partial^2 \zeta_1(z,t)}{\partial z^2}$$

4. Application: state observer design for parameter identification

This section presents a possible application of the formerly discussed Liénard-type models. The application is on estimation issues, for which a so-called *observer approach* is proposed [22], that is on-line algorithms allowing the recovery of unknown variables from the use of the model together with driving and measured variables. The appropriate observer is first presented, and application examples for parameter estimation in a pipeline are then given.

4.1. Observer tool

For a dynamical system described by

$$\begin{aligned} \dot{\xi}(t) &= A(y(t))\,\xi(t) + B(y(t), u(t)) \\ y(t) &= C\,\xi(t) \end{aligned} \tag{32}$$

where A, B, C are known functions, while $\xi(t)$ denotes the state vector, $u(t)$ some known driving input, and $y(t)$ the measured output, an *exponential observer* can take the following form [23]:

$$\dot{\hat{\xi}}(t) = A(y(t))\,\hat{\xi}(t) + B(y(t), u(t)) - S^{-1}(t)C^{\mathrm{T}}(C\hat{\xi}(t) - y(t)) \tag{33}$$

$$\dot{S}(t) = -\lambda S(t) - A^{\mathrm{T}}(y(t))S(t) - S(t)A(y(t)) + C^{\mathrm{T}}C, \quad \text{for } \lambda > 0, \text{and } S(0) > 0 \tag{34}$$

in the sense that the error $\hat{\xi}(t) - \xi(t)$ can exponentially decay to zero as t goes to infinity.

In this case, the rate of decay is tunable by means of parameter λ.

The exponential convergence is guaranteed under an appropriate excitation condition on $u(t), y(t)$ given by:

$$\begin{aligned} &\exists T, \beta', \alpha' > 0 : \\ &\beta' I \geq \int_t^{t+T} \Psi_v^{\mathrm{T}}(\tau, t)\, C^{\mathrm{T}} C \Psi_v(\tau, t)\, \mathrm{d}\tau \geq \alpha' I, \quad \forall t \geq t_0 \end{aligned} \tag{35}$$

where I is the identity matrix and Ψ_v denotes the transition matrix satisfying

$$\begin{cases} \dfrac{\mathrm{d}}{\mathrm{d}\tau}\Psi_v(\tau, t) = A(v(\tau))\Psi_v(\tau, t) \\ \Psi_v(t, t) = I \end{cases}$$

In Section 4, it was shown that a Liénard system with functions F_0, G_0 *linearly parameterized* with respect to some parameter vector θ can take the structure (6). At this point, an observer for both state and parameter estimation can be designed with the structure given in Eq. (33), provided that the system (6) be set in the adequate form, by considering

$$\xi(t) := \begin{bmatrix} x(t) \\ \theta \end{bmatrix} \tag{36}$$

Here $\xi(t) \in \mathbb{R}^{n+n_\theta}$ denotes the augmented state vector of the new augmented system, if $x(t) \in \mathbb{R}^n$ and $\theta \in \mathbb{R}^{n_\theta}$:

$$\begin{aligned} \dot{\xi}(t) &= \underbrace{\begin{pmatrix} A_o & \Phi(y(t)) \\ 0 & 0 \end{pmatrix}}_{A(y(t))} \xi(t) + \underbrace{\begin{pmatrix} \varphi(y(t), u(t)) \\ 0 \end{pmatrix}}_{B(y(t),u(t))} \\ y(t) &= C\xi(t) \end{aligned} \tag{37}$$

where $C = (C_0 \quad 0)$ and zero submatrices of appropriate dimensions.

4.2. Example: estimation of wave speed and friction or inner diameter

Pipeline parameters naturally change as time goes by. Therefore, identification algorithms that update the actual values are always required to adjust control or monitoring systems. In this work, by taking advantage of the linearized Liénard type-model of the pipeline expressed by (31), an observer is proposed to estimate the inner diameter, the wave speed and the friction factor. To do that, the following spatial-discrete version of such a equation in terms of the flow rate is considered:

$$\begin{aligned} \dot{Q}_i^a(t) &= Q_i^b(t) - \alpha Q_i^a(t) \\ \dot{Q}_i^b(t) &= \gamma \nabla^2 Q_i^a(t) \end{aligned} \tag{38}$$

where $\nabla^2 Q_i^a(t) \approx (Q_{i-1}^a(t) - 2Q_i^a(t) + Q_{i+1}^a(t))/\Delta z^2$, Δz is the spatial step of the discretization and i is the spatial discretization index. Recall that $\alpha = \mathcal{R}/\mathcal{L} = f\,|Q_0|\,/A_r\phi$ refers to a dissipation coefficient, and $\gamma = 1/\mathcal{L}\mathcal{C} = b^2$ refers to a diffusion coefficient.

Now when $\theta = [\alpha \ \gamma]^{\mathrm{T}}$ is the parameter vector to be estimated, then the extended vector of the system to be used for the observer design (according to (36)) becomes $\xi(t) = [\xi_1(t), \xi_2(t), \xi_3(t), \xi_4(t)]^{\mathrm{T}} = [Q_{\mathrm{in}}^a(t), Q_{\mathrm{in}}^b(t), \alpha, \gamma]^{\mathrm{T}}$. This requires that available measurements, as well as input variables, be specified. Here it is assumed that flow rates at the pipeline positions $i-1$, i, and $i+1$ are available along the pipeline: Q_{i-1}^a, Q_i^a and Q_{i+1}^a with $y(t) = Q_i^a(t)$. Finally, by considering this scenario, model (38) can be rewritten in the form (37) as

$$\begin{aligned} \dot{\xi}(t) &= \begin{bmatrix} 0 & 1 & -y & 0 \\ 0 & 0 & 0 & \nabla^2 y \\ 0 & 0 & 0 & 0 \\ 0 & 0 & 0 & 0 \end{bmatrix} \xi(t) \\ y(t) &= [1 \quad 0 \quad 0 \quad 0]\,\xi(t) \end{aligned} \tag{39}$$

and an observer for both state and parameter estimation can be designed by (33). In particular, the estimation of $\xi_4(t)$ gives the wave speed and that of $\xi_3(t)$ gives the friction coefficient if the inner diameter is known or the inner diameter if the friction is known.

4.3. Example: estimation of friction and equivalent length in a pipeline

In practice, the existence of fittings such as tees, reducers or elbows cause pressure loss or resistance, which can be a drawback for monitoring or diagnosis methods if they are not well known, or regularly changing under upkeep operations. As a remedy to this situation, a very important concept in fluid dynamics can be used: the *equivalent length*, which is the length of an imaginary straight duct that would have a frictional head loss equal to a more complex pipeline with valves and fittings.

To find the equivalent length, a virtual substitution of each fitting by an equivalent straight pipe segment should be done. This task involves the use of the so-called loss coefficient of a particular fitting; see Chapter 5 in [24]. This parameter can be found in manufacturer data sheets and normally is denoted by K. The provided K value, however, is usually larger than the real one in order to provide a security margin when a pipeline system is designed.

To have a more precise value of K for each accessory, the authors in [25] proposed a state observer for its online estimation. More recently, in [1], a state observer for estimating the friction factor and the equivalent length of a pipeline was developed. Such an observer was designed from a discrete version of the flow rate model given by Eq. (17); it requires three flow measurements along the pipeline: for instance, two measurements at each boundary and another one in between.

The observer works well according to test results; however, it is always better to have algorithms that work with fewer sensors. A state observer is then proposed that simultaneously estimates the equivalent length and the friction of a pipe by using only boundary measurements. For the design of such an observer, the ensuing steps are carried out.

Firstly, let us consider model (17) for the pipe dynamics. Let us further assume that the pipe flow is driven by pressure heads at the boundaries. Let us then differentiate Eq. (22) with respect to space to get

$$\frac{\partial^2 Q(z,t)}{\partial z^2} = -\frac{gA_r}{b^2}\frac{\partial \dot{H}(z,t)}{\partial z} \tag{40}$$

where $\dot{H}$ stands for $\partial H/\partial t$.

Injecting this in model (17) subsequently yields:

$$\begin{aligned}\frac{\partial Q^a(z,t)}{\partial t} &= Q^b(z,t) - \frac{f}{2\phi A_r}|Q^a(z,t)|Q^a(z,t)\\ \frac{\partial Q^b(z,t)}{\partial t} &= -gA_r\frac{\partial \dot{H}(z,t)}{\partial z}\end{aligned} \tag{41}$$

If Eq. (41) is discretized in space by using both the forward and backward finite difference methods, respectively, one gets the following ODE systems:

$$\begin{aligned}\dot{Q}_i^a(t) &= Q_i^b(t) - \frac{f}{2\phi A_r}|Q_i^a(z,t)|Q_i^a(z,t)\\ \dot{Q}_i^b(t) &= -gA_r\frac{\dot{H}_{i+1}(t) - \dot{H}_i(t)}{\Delta z}, \qquad \forall i = 1,2,..,N\end{aligned} \tag{42}$$

$$\begin{aligned}\dot{Q}_i^a(t) &= Q_i^b(t) - \frac{f}{2\phi A_r}|Q_i^a(z,t)|Q_i^a(z,t)\\ \dot{Q}_i^b(t) &= -gA_r\frac{\dot{H}_i(t) - \dot{H}_{i-1}(t)}{\Delta z}, \qquad \forall i = 1,2,..,N\end{aligned} \tag{43}$$

where Δz is the space step and N is the total number of discretized sections.

If one sets $\Delta z = L_{eq}$, $Q_i^a(t) = Q_{\text{in}}(t)$, $\dot{H}_i(t) = \dot{H}_{\text{in}}(t)$ and $\dot{H}_{i+1}(t) = \dot{H}_{\text{out}}(t)$, system (42) becomes

$$\begin{aligned}\dot{Q}_{\text{in}}^a(t) &= Q_{\text{in}}^b(t) - \frac{f}{2\phi A_r}|Q_{\text{in}}^a(t)|Q_{\text{in}}^a(t)\\ \dot{Q}_{\text{in}}^b(t) &= gA_r\frac{\dot{H}_{\text{in}}(t) - \dot{H}_{\text{out}}(t)}{L_{eq}}, \qquad \forall i = 1,2,..,N\end{aligned} \tag{44}$$

Finally, if one defines $\xi(t) = [\xi_1(t), \xi_2(t), \xi_3(t), \xi_4(t)]^{\text{T}} = [Q_{\text{in}}^a(t), Q_{\text{in}}^b(t), f, 1/L_{\text{eq}}]^{\text{T}}$ as a state vector and $y(t) = \xi_1(t)$ as the output, the following extended system is obtained:

$$\begin{aligned}\dot{\xi}(t) &= \begin{pmatrix} 0 & 1 & -\dfrac{1}{2\phi A_r}(|\xi_1(t)|\xi_1(t)) & 0\\ 0 & 0 & 0 & gA_r\left(\dot{H}_{\text{in}}(t) - \dot{H}_{\text{out}}(t)\right)\\ 0 & 0 & 0 & 0\\ 0 & 0 & 0 & 0 \end{pmatrix}\xi(t)\\ y(t) &= \xi_1(t)\end{aligned} \tag{45}$$

which is suitable to design an observer with the form given by Eq. (33) as soon as $\dot{H}_{\text{in}}(t), \dot{H}_{\text{out}}(t)$ are known. Notice that $Q_{\text{out}}(t)$ together with system (43) could also be used instead of $Q_{\text{in}}(t)$ and system (42) to perform the estimation.

5. Tests

5.1. Simulation tests

Hereafter the observer constructed from the extended system given by (39) is evaluated. The pipeline behavior is simulated via a Finite-Difference approximation of equations (10)–(9) over $n = 50$ sections. The spatial step size is thus $\Delta z = L/n = 4.0033$ [m]. All simulations were done within the MATLAB© environment. The step time of the solver (ODE3) is set to $\Delta t = 0.001$ [s], allowing us to satisfy the Courant condition. Pressures at the pipe ends, $H_{\text{in}}(t)$ and $H_{\text{out}}(t)$, are considered as boundary conditions to approximate (10)–(9). Finally, the physical parameters of the simulated pipeline are displayed in Table 2.

Table 2
Physical parameters.

Parameter	Value	Parameter	Value
L	200.16 [m]	b	1284 [m/s]
ϕ	0.1016 [ ]	f	0.022
$\mathcal{R}$	6.4141	$\mathcal{L}$	≈ 12.5734
$\mathcal{C}$	$\approx 4.8240 \times 10^{-8}$	q_0	≈ 0.019130 [m^3/s]

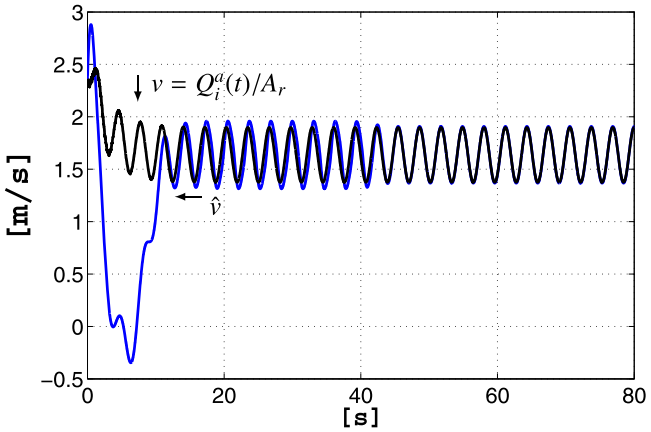

Fig. 1. Velocity v and its estimation $\hat{v}$.

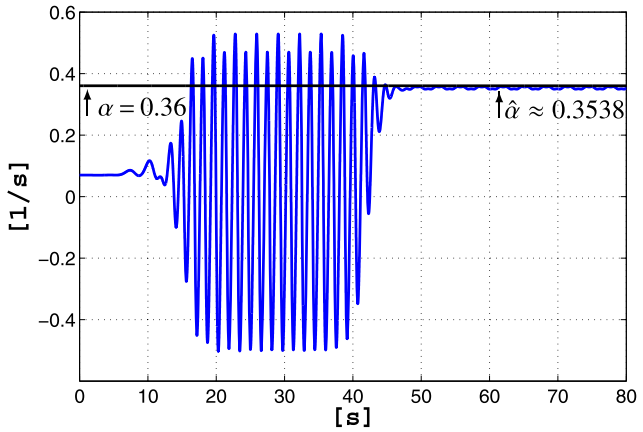

Fig. 2. α and its estimation $\hat{\alpha}$.

The results obtained from the estimation are presented as follows: in Fig. 1, the estimated velocity $\hat{Q}^a(t)/A_r$ is shown. In Figs. 2 and 3, the estimation of parameters $\hat{\theta} = [\hat{\alpha} \;\; \hat{\gamma}]^{\mathrm{T}}$ are presented with respect to their actual values.

In addition, the estimation of θ allows us to estimate either the pipeline diameter ϕ or the friction coefficient f. If the equilibrium flow rate Q_0 is known, as well as the friction coefficient f and the estimates $\hat{\alpha}$, then an estimate of the inner diameter ϕ can be computed as

$$\hat{\phi} = \left(\frac{4 f Q_0}{\hat{\alpha} \pi} \right)^{1/3} \tag{46}$$

In Fig. 4, this estimated diameter is shown; it converges to 0.1023 [m], with an estimation error of 0.6889%.

If the equilibrium flow rate Q_0 is known as well as the inner diameter ϕ, then $\hat{\alpha}$ permits an estimate for the friction coefficient as

$$\hat{f} = \left(\frac{\pi \phi^3 \hat{\alpha}}{4 Q_0} \right) \tag{47}$$

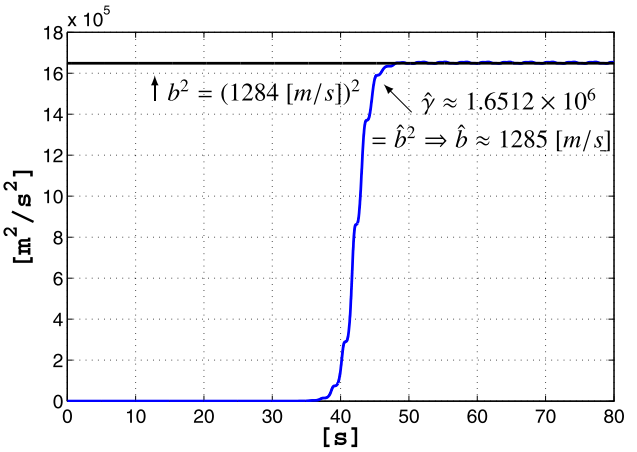

Fig. 3. γ and its estimation $\hat{\gamma}$.

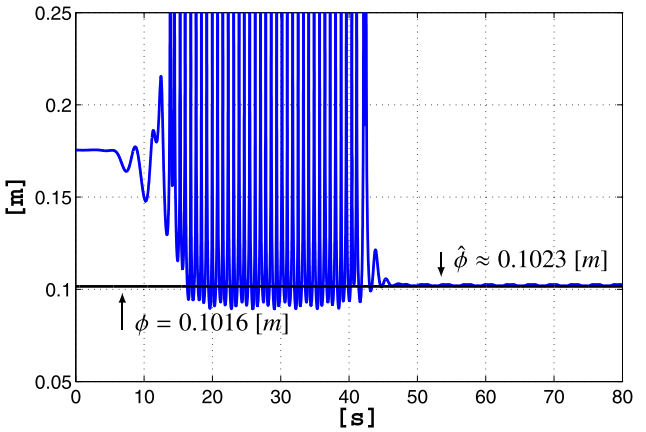

Fig. 4. ϕ and its estimation $\hat{\phi}$.

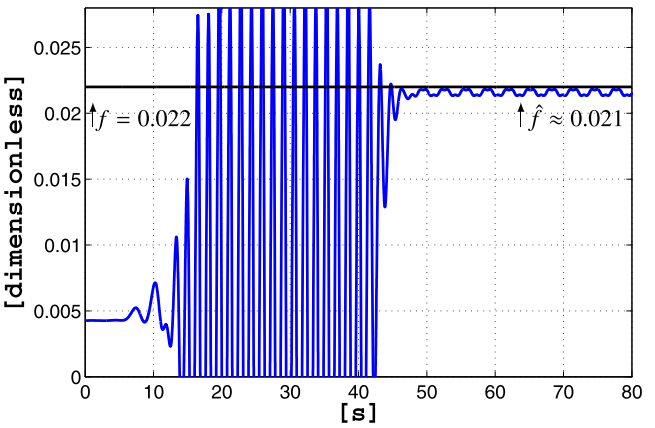

Fig. 5. f and its estimation $\hat{f}$.

In Fig. 5, the estimated friction coefficient is shown; it converges to 0.0216, with an estimation error of 1.8181%.

The estimation errors can be caused by the use of a linearized version of the dynamical model, but the estimates are pretty successful.

List of components			
Identifier	Component	Identifier	Component
E-1	Reservoir	P-1	Pressure sensor
E-2	Pump	P-2	Pressure sensor
V-1	Valve	F-1	Flow sensor
V-2	Valve	F-2	Flow sensor
V-3	Valve	E-3	Reservoir
V-4	Valve	E-4	Pump

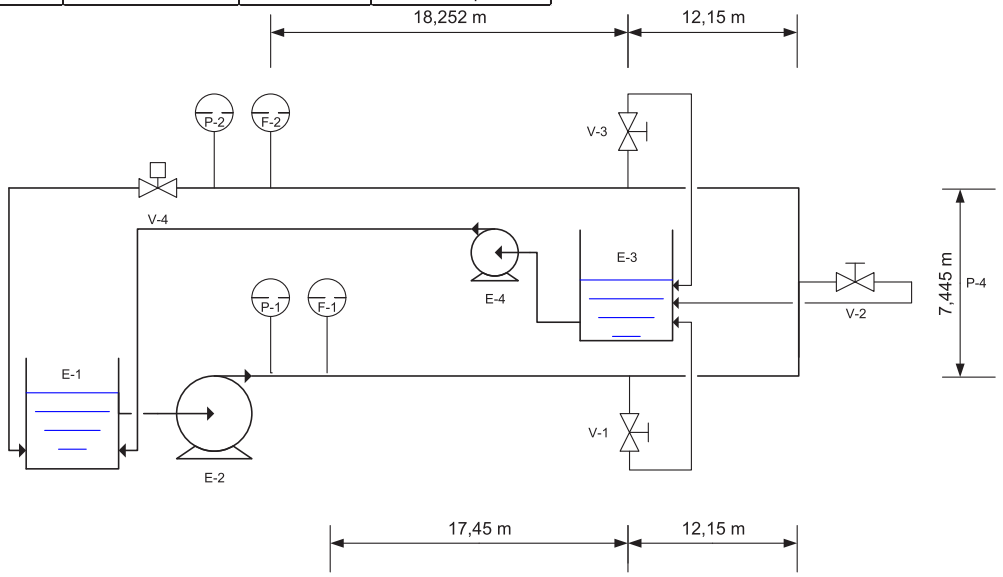

Fig. 6. Pipeline prototype scheme.

Table 3
Physical parameters, CINVESTAV prototype.

Parameter	Value	Parameter	Value
L_{eq}	85.5 [m]	b	393 [m/s]
ϕ	0.06271 [m]	f	0.017

5.2. Experimental tests

In this section, some experimental results are presented in order to evaluate the observer's performance given by Eq. (33) and based on the extended system (45). Here the prototype, which was built at the CINVESTAV-Guadalajara has been considered. The prototype is equipped, among other things, with a 5 [HP] centrifugal pump (Pump 1), which provides the energy needed to transport the water inside the pipeline. The pump is controlled by a Variable-Frequency Drive (VFD) between 0 and 60 Hz, which controls the rotational speed of the pump motor by a variation of the AC frequency. The instrumentation consists of flow sensors (FTs) as well as of pressure ones (PTs) installed at both ends of the pipeline; see Fig. 6. The flow rate is measured by using electromagnetic flowmeters (Endress Hauser, mod. Proline Promag 10P). The pressure head is measured by using a piezometric diaphragm sensor (Endress Hauser, mod. Cerabar M). A full description is given in [26].

On the other hand, a database is acquired from flow rate and pressure head measurements, which are obtained at a sampling rate of 100 Hz, by employing a LabVIEW© environment through data acquisition card NI USB-6229. The implementation was done offline in a MATLAB© environment. The main pipeline parameters are summarized in Table 3.

The experiment was performed as follows: Pump 1 is started in a steady state operation during the first 80 s approximately. After that, it begins to operate in some unsteady state, namely, a sine-like pressure signal is introduced, exactly like a persistent input condition in the sense of Eq. (35). This sine signal was experimentally obtained by setting up the pump controller as follows:

$$\begin{cases} VFD(t) = 60\ [\text{Hz}], \ \text{for}\ \forall\, t \leq 80\ [\text{s}] \\ VFD(t) = 50 + 5\sin(2.7313\, t)\ [\text{Hz}], \ \text{for}\ \forall\, t > 80\ [\text{s}] \end{cases}$$

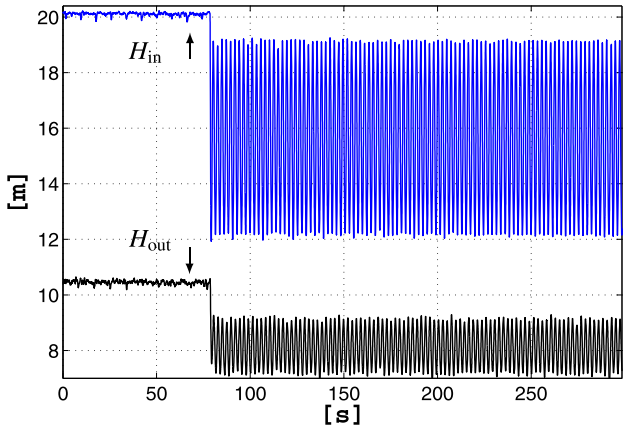

Fig. 7. Pressure heads.

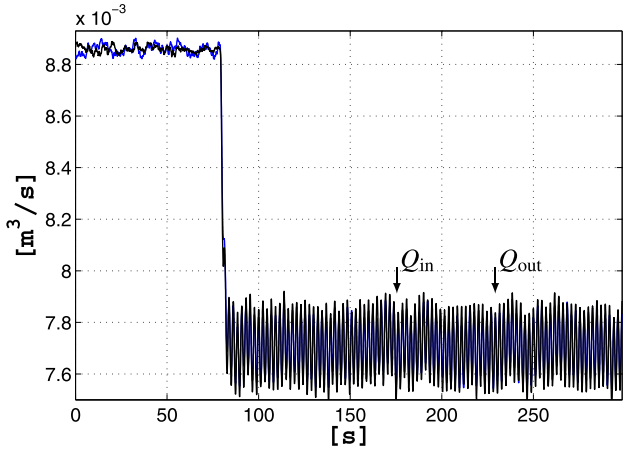

Fig. 8. Flow rates.

This signal is characterized in pressure terms as follows:

$$\begin{cases} H_{\text{in}}(t) \approx 20.12 \text{ [m]}, \ H_{\text{out}}(t) \approx 10.48 \text{ [m]}, \ \text{for } \forall\, t \leq 80 \text{ [s]} \\ H_{\text{in}}(t) \approx 15.645 + 3.455 \sin(2.7313t) \text{ [s]}, H_{\text{out}}(t) \approx 8.2105 + 0.9335 \sin(2.6180\, t) \text{ [m]}, \ \text{for } \forall\, t > 80 \text{ [s]} \end{cases}$$

By defining a new extended state vector $\xi(t) = [\xi_1(t), \xi_2(t), \xi_3(t), \xi_4(t)]^{\mathrm{T}} = [Q_{\text{in}}^a(t),\, Q_{\text{in}}^b(t),\, f,\, 1/L_{eq}]^{\mathrm{T}}$, the observer was tuned with $\lambda = 7$ and initialized with the following conditions:

$$\xi(0) = [\xi_1(0), \xi_2(0), \xi_3(0), \xi_4(0)]^{\mathrm{T}} = [0.005, 0.005, 0.025, 1/300]^{\mathrm{T}},\ S(0) = \text{diag}(1, 1, 1, 1)$$

The derivatives of the boundary pressures were calculated by using the URED algorithm proposed in [27], which was tuned with $k_1 = 0.99$ and $k_2 = k_1^2$. Previously, these signals as well as the flow rate measurements were filtered by using a third-order Butterworth low-pass filter with a passband edge frequency of 7 [rad/s].

Hereafter, it is highlighted how this persistent input condition allows the estimation of both the equivalent pipeline length and the friction coefficient properly. In Figs. 7 and 8, the pressure head and the flow rate measurements are displayed, respectively.

Fig. 9 then shows the friction factor estimation as well as the one calculated by using the so-called Swamee–Jain equation (48) [28]. Notice that while the persistent input condition is absent for $t \leq 80$ [s], the observer does not converge. For $t > 80$ [s], however, the observer begins to estimate the friction factor, and estimation is indeed successfully achieved:

$$f = \frac{0.25}{\left[\log_{10}\left(\dfrac{\varepsilon}{3.7\phi} + \dfrac{5.74}{Re^{0.9}}\right)\right]^2} \tag{48}$$

In Fig. 10, it can be seen the calculated equivalent length by using the Darcy–Weisbach equation (49) [29], which is oscillatory-like for $t > 80$ [s] because of the persistent input condition $u(t)$, as expected. This is explained as follows: the

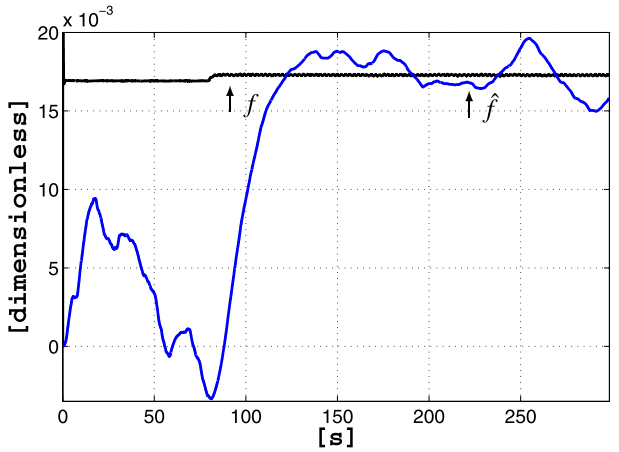

Fig. 9. f and its estimation $\hat{f}$.

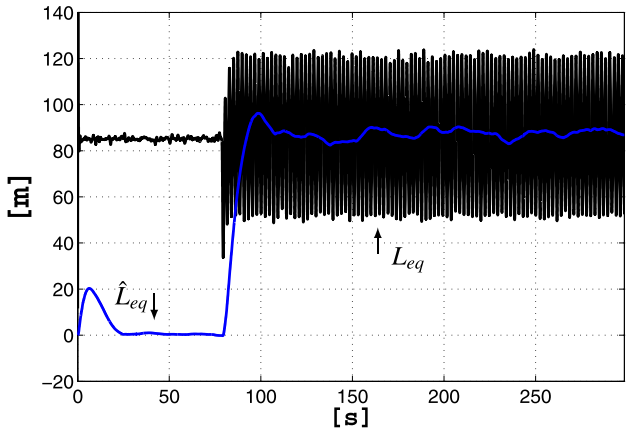

Fig. 10. L_{eq} and its estimation $\hat{L}_{eq}$.

empirical Darcy–Weisbach equation considers an average flow rate in order to estimate the head losses along a pipeline (steady state). However, when the persistent input arrives, this assumption is not fulfilled, because the used variables (pressure and flow rate) are in unsteady state. Therefore one cannot rely on Darcy–Weisbach equation when an oscillatory regime is present. Finally, notice that the estimated equivalent pipeline length coincides with the one calculated before the oscillations start, as desired:

$$L_{\text{eq}} = \frac{\Delta H \left(\phi^5 \pi^2 g\right)}{8 f Q^2} \tag{49}$$

6. Conclusions

In this article, the derivation of Liénard-type models for fluid transmission line dynamics has been presented. The interest of this model for estimation purposes has been emphasized by presenting a related exponential boundary observer that estimates the friction and the equivalent length of a pipeline. Simulation and experimental tests have finally been provided to illustrate the good performance of the proposed observer. The design of observers based on the infinite-dimensional model are considered to be presented in future works.

Acknowledgements

The authors acknowledge the financial support from DGAPA of Universidad Nacional Autónoma de México through the following project: IT100716. The authors also thank Instituto de Ingeniería and Facultad de Ingeniería of Universidad Nacional Autónoma de México for financing the project “Procesamiento digital de señales para la supervisión de líneas de transmisión de fluidos”.

Appendix A. Supplementary material

Supplementary material related to this article can be found online at http://dx.doi.org/10.1016/j.crme.2016.04.004.

References

[1] L. Torres, G. Besançon, C. Verde, Liénard type model of fluid flow in pipelines: application to estimation, in: 12th International Conference on Electrical Engineering, Computing Science and Automatic Control, Mexico City, Mexico, IEEE, 2015, pp. 148–153.
[2] S. Beck, N. Williamson, N. Sims, R. Stanway, Pipeline system identification through cross-correlation analysis, Proc. Inst. Mech. Eng., E J. Process Mech. Eng. 216 (3) (2002) 133–142.
[3] J. Yang, Y. Wen, P. Li, Leak location using blind system identification in water distribution pipelines, J. Sound Vib. 310 (1) (2008) 134–148.
[4] A.C. Zecchin, L.B. White, M.F. Lambert, A.R. Simpson, Parameter identification of fluid line networks by frequency-domain maximum likelihood estimation, Mech. Syst. Signal Process. 37 (1) (2013) 370–387.
[5] V. Ibarra-Junquera, H. Rosu, PI-controlled bioreactor as a generalized Liénard system, Comput. Chem. Eng. 31 (3) (2007) 136–141.
[6] B.V. der Pol, J.V. der Mark, The heartbeat considered as a relaxation oscillation, and an electrical model of the heart, Philos. Mag. Ser. 7 6 (38) (1928) 763–775.
[7] H.N. Moreira, Liénard-type equations and the epidemiology of malaria, Ecol. Model. 60 (2) (1992) 139–150.
[8] J. Nagumo, S. Arimoto, S. Yoshizawa, An active pulse transmission line simulating nerve axon, Proc. IRE 50 (10) (1962) 2061–2070.
[9] R. FitzHugh, Impulses and physiological states in theoretical models of nerve membrane, Biophys. J. 1 (6) (1961) 445–466.
[10] A.L. Hodgkin, A.F. Huxley, A quantitative description of membrane current and its application to conduction and excitation in nerve, J. Physiol. 117 (4) (1952) 500–544.
[11] X.C. Huang, Limit cycles in a continuous fermentation model, J. Math. Chem. 5 (3) (1990) 287–296.
[12] P. Holmes, D. Rand, Phase portraits and bifurcations of the nonlinear oscillator: $\ddot{x} + \alpha\dot{x} + \gamma x^2\dot{x} + \beta x + \delta x^3 = 0$, Int. J. Non-Linear Mech. 15 (6) (1980) 449–458.
[13] P. Omari, G. Villari, F. Zanolin, A survey of recent applications of fixed point theory to periodic solutions of the Liénard equation, in: Fixed Point Theory and Its Applications, vol. 72, American Mathematical Society, Providence, RI, USA, 1988, pp. 171–178.
[14] P. Yu, M. Han, Limit cycles in generalized Liénard systems, Chaos Solitons Fractals 30 (5) (2006) 1048–1068.
[15] S. Lynch, Liénard systems and the second part of Hilbert's Sixteenth problem, Nonlinear Anal. 30 (3) (1997) 1395–1403.
[16] T. Slight, B. Romeira, L. Wang, J.M.L. Figueiredo, E. Wasige, C.N. Ironside, A Liénard oscillator resonant tunnelling diode–laser diode hybrid integrated circuit: model and experiment, IEEE J. Quantum Electron. 44 (12) (2008) 1158–1163.
[17] E. Abd-Elrady, T. Soderstrom, T. Wigren, Periodic signal modeling based on Liénard's equation, IEEE Trans. Autom. Control 49 (10) (2004) 1773–1781.
[18] A. Liénard, Étude des oscillations entretenues, Rev. Gén. Électr. 23 (1928) 901–954.
[19] G. Besançon, A. Voda, Observer-based parameter estimation in Liénard systems, in: Adaptation and Learning in Control and Signal Processing, ALCOSP 2010, Anatolia, Turkey, 2010.
[20] G. Besançon, A. Voda, G. Jouffroy, A note on state and parameter estimation in a Van der Pol oscillator, Automatica 46 (2010) 1735–1738.
[21] M.H. Chaudhry, Applied Hydraulic Transients, Van Nostrand Reinhold, New York, 1979.
[22] G. Besançon, Nonlinear Observers and Applications, Springer, 2007.
[23] G. Besançon, G. Bornard, H. Hammouri, Observer synthesis for a class of nonlinear control systems, Eur. J. Control 2 (1996) 176–192.
[24] J.A. Roberson, J.J. Cassidy, M.H. Chaudhry, Hydraulic Engineering, Wiley, New York, 1998.
[25] A. Navarro, O. Begovich, G. Besançon, Calibration of fitting loss coefficients for modelling purpose of a plastic pipeline, in: Proc. 16th Conference on Emerging Technologies & Factory Automation (ETFA), IEEE, 2011, pp. 1–6.
[26] J. Delgado-Aguiñaga, G. Besançon, O. Begovich, J. Carvajal, Multi-leak diagnosis in pipelines based on extended Kalman filter, Control Eng. Pract. 49 (2016) 139–148.
[27] E. Cruz-Zavala, J.A. Moreno, L.M. Fridman, Uniform robust exact differentiator, IEEE Trans. Autom. Control 56 (11) (2011) 2727–2733.
[28] P.K. Swamee, A.K. Jain, Explicit equations for pipe-flow problems, J. Hydraul. Div. 102 (5) (1976) 657–664.
[29] C. Mataix, Mecánica de Fluidos Y Máquinas Hidráulicas, El Castillo, 1986.